Pt(111) Reconstruction Induced by Enhanced Pt Gas-Phase Chemical Potential

Michael Bott, Michael Hohage, Thomas Michely, and George Comsa
Institut für Grenzflachenforschung und Vakuumphysic, Kernforschungsanlage Jülich GmbH, Forschungszentrum Jülich, P.O. Box 1913, D-5170 Jülich, Germany
(Received 24 August 1992)

Large terraces of the Pt(111) surface are shown to reconstruct in the presence of a Pt gas-phase environment down to 400 K. The lifting of the reconstruction in the absence of the Pt gas phase is kinetically hindered up to 700 K. The main features of the reconstruction network as seen by the scanning tunneling microscope correspond to those inferred from x-ray scattering for the high-temperature (> 1330 K) spontaneous Pt(111) reconstruction. The parallel double corrugation lines forming the network have basically the same structure as those seen on the reconstructed Au(111) surface.

PACS numbers: 68.35.Rh, 61.16.Ch, 64.70.Kb, 82.65.Dp

The unreconstructed (111) surface of the fcc metals is considered to be particularly stable. Gold has been believed for a long time to be the only exception [1]. However, recently Sandy *et al.* [2] reported that at high temperature Pt(111) also reconstructs, but that below 1330 K the unreconstructed phase is stable. The findings reported below demonstrate that in the presence of a supersaturated Pt gas-phase environment, the reconstructed phase of Pt(111) becomes the stable one down to low temperatures. This appears to be a new way to stabilize the reconstructed phase.

The structure of the reconstruction of Au(111) has been investigated by various methods and was discussed recently [1] in great detail in a scanning tunneling microscopy (STM) study. The reconstructed surface can be described by a "stacking-fault-domain model involving periodic transitions from fcc to hcp stacking of top-layer atoms." The transition regions which board the hcp domain appear as bright parallel double straight lines 27 Å apart and 0.20 ± 0.05 Å high running along the $[11\bar{2}]$ direction. Each pair of lines contains an extra row of atoms (i.e., one extra row for each 22 substrate rows) leading to a local uniaxial compression in the $[1\bar{1}0]$ direction and thus to a 4.5% higher density of Au atoms in the top layer. These double lines form a periodic structure with a superlattice constant of 63 Å (22×2.884 Å) in the $[1\bar{1}0]$ direction. The line pairs do not cross but bend by $\pm 120°$ each 250 Å, forming a zigzag pattern. They end in a kind of U-turn so that the hcp and fcc domains are fully separated by the transition regions.

The structure of the reconstructed Pt(111) surface, stable only above 1330 K, is known in less detail so far. From their x-ray scattering data, Sandy *et al.* [2] inferred that the reconstructed surface is isotropically compressed, forming a disordered arrangement of discommensurate regions which separate fcc from hcp regions. The ratios of the corresponding fractional areas are 0.12:0.70:0.18. With increasing temperature the compression of the surface layer and the hexagonal order of the discommensurate regions appears to increase, whereas the translational correlation length appears to decrease down to 100 Å.

The reconstruction of the Pt(111) surface reported here is induced down to 400 K by the presence of a supersaturated Pt gas-phase environment. The STM images shown below demonstrate that the structure of this reconstructed surface may correspond to that of the high-temperature reconstructed Pt(111) surface. Some of its constituents, the double lines and even the U-turns, are qualitatively and quantitatively equivalent to those found on the reconstructed Au(111) surface. However, at variance with the latter case, on the low-temperature Pt(111) reconstruction the double lines cross, forming a network structure.

In a theoretical study Needs, Godfrey, and Mansfield [3] concluded that there are three main factors determining the stability of the (111) surfaces of Al, Ir, Pt, and Au: (1) their tendency to have shorter bond lengths (i.e., higher density) within the surface plane; (2) the energy changes associated with transferring excess atoms into the surface layer in order to increase its density; and (3) the reduced bonding energy to the substrate of a compressed reconstructed layer which is at least partially incommensurate. Obviously (1) is the driving force of the reconstruction, while (2) and (3) tend to stabilize the unreconstructed phase.

Estimating the balance between these factors, Needs, Godfrey, and Mansfield [3] find that the (111) surfaces of Ir, Pt, and Au "are close to an instability towards adding atoms to the surface." The reconstruction of the Au(111) surface outlined above, which appears to be the stable phase in the whole temperature range 300–1250 K investigated so far, supports this conclusion.

The Pt(111) surface seems to be a borderline case. Indeed as mentioned above Sandy *et al.* [2] found that around 1330 K there is a change in the stability of the surface phase. These authors ascribe the stability of the reconstruction at high temperatures to the fact that factor (3), which tends to stabilize the unreconstructed phase, becomes less important: Because the corrugation of the bonding potential is less pronounced at high temperature, the energy difference between a commensurate and an incommensurate arrangement of the top layer is

lowered.

The stabilization of the reconstructed phase down to 400 K by providing a highly supersaturated Pt gas phase above the Pt(111) surface during Pt deposition, which is reported here, can also be understood on the basis of the considerations of Needs, Godfrey, and Mansfield. Indeed, they show that factor (2) which arises from the energy changes associated with transferring excess atoms into the surface, contains as an additional term "the negative of the chemical potential of the particle reservoir" which "consists of the kink sites at atomic steps on the surface." During the deposition of Pt atoms from the gas phase we are in fact connecting an additional particle reservoir with a much larger chemical potential. Because the binding energy of a Pt adatom is substantially less than that of a Pt kink atom, the presence of the Pt gas phase and thus of an excess of Pt adatoms not only increases the availability of atoms for transfer into the surface but also decreases the energy cost per atom. In this way the effect of factor (2) which stabilizes the unreconstructed phase is appreciably reduced and the balance of the three factors inclines in favor of the reconstructed phase.

An additional remark is in order here. Obviously, the highly supersaturated Pt gas phase influences the stability of the Pt(111) surface by creating a supersaturated two-dimensional Pt adatom lattice gas on the surface. The actual Pt adatom density is of course not homogeneous. In the presence of a supersaturated Pt gas phase, the steps and in particular the kinks present on the surface act as sinks for Pt adatoms. The supersaturation of the Pt adatom lattice gas is reduced in the vicinity of the steps. As a consequence the low-temperature reconstruction reported here is observed mainly on large terraces at some distance from the steps present.

The experiments were performed in a UHV chamber equipped with Auger-electron spectroscopy, low-energy electron diffraction, a sputtering ion gun, a Pt deposition system, and a variable temperature STM. The various components are described in detail elsewhere [4–6]. The usual procedure was as follows: We deposited 0.04–0.8 monolayer (ML) of Pt at rates in the range 1.5×10^{-4}–1×10^{-2} ML/s (deposition times in the range 10–1500 s) and fixed sample temperatures, $400\ \mathrm{K} < T_s < 690\ \mathrm{K}$. When the desired deposited amount had been reached, the Pt deposition beam and the sample heating were turned off simultaneously. The frozen-in reconstruction was measured with the STM at room temperature. We have performed more than 100 experiments (half of them without deposition) on two different Pt(111) crystals: We *never* observed reconstruction without previous Pt deposition, but always after deposition under the conditions stated above. The fractional area covered by the reconstruction appears to increase with the crystal temperature during deposition, reaching $> 80\%$ on the largest terraces. At lower temperature a higher deposition rate is needed to induce significant reconstruction. We have checked carefully whether the presence of minute amounts of adsorbates, in particular of "subsurface" oxygen [7], might induce the reconstruction. From the always negative result we inferred that the reconstruction is a property of the clean surface. The reconstruction once formed keeps its shape even in the absence of the supersaturated Pt gas phase if the surface temperature is below 700 K: It is in a kinetically hindered metastable phase. Above 700 K the reconstruction fades away.

In the wide range STM image in Fig. 1 the higher very large terrace is almost (except for the depletion zone near the preexistent step and the immediate vicinity of the islands) fully covered by the network of the reconstruction while the lower terrace (upper left corner) is unreconstructed. The network has a honeycomblike structure with a more or less hexagonal symmetry of the unit cell and orientational order over large areas. An interesting aspect in Fig. 1 is the density of the monatomic high islands: While on the unreconstructed lower terrace (only partially shown) the island density has a "normal" value corresponding to the deposition temperature and rate [6]; on the reconstructed surface there is, besides large islands with "normal" density, an approximately one order larger density of small islands. The increase of the nucleation probability after the surface has been reconstructed indicates substantially slower Pt adatom migration on the reconstructed surface.

The pattern of the reconstructed surface is shown in more detail in Fig. 2. It consists mainly of hexagonally shaped "unit cells" with linear dimensions between 100 and 300 Å. The sides of the hexagon are bright parallel double lines (DL) 23 ± 2 Å apart and 0.25 ± 0.04 Å high, running along the $\langle 11\bar{2} \rangle$ directions, i.e., within the

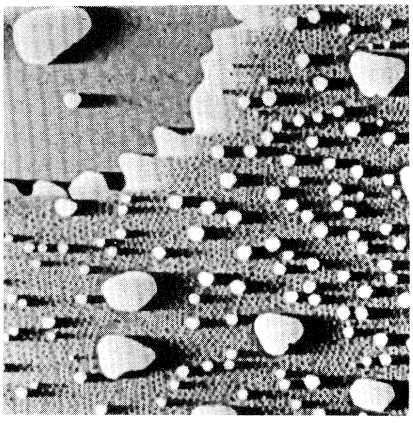

FIG. 1. STM image of 5700 Å × 5700 Å taken after deposition of 0.1 ML at 690 K at a deposition rate of 3×10^{-3} ML/s. The image is represented with illumination at near glancing incidence from the left.

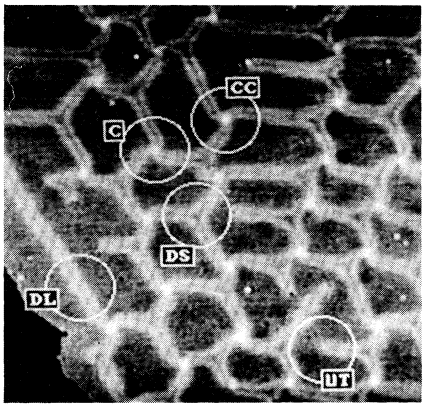

FIG. 2. STM image of 1000 Å×1000 Å size after deposition of 0.3 ML at 630 K at a deposition rate of 3×10^{-3} ML/s. The higher terrace covering almost the entire image is reconstructed while the lower one (lower left corner) is unreconstructed.

error limits, identical to the double lines, which are the basic element of the Au(111) reconstruction. At the corners of the hexagons, where three double lines meet, starlike features are formed. These are novel features not seen in the Au(111) reconstruction where the double lines do not meet. There are two types of stars: (1) stars with a lower lying dark center (DS) and (2) stars with a raised (0.55 ± 0.08 Å) bright center which always form alternatively the six corners of the hexagons. The double lines forming the three rays of the dark stars are always straight and are separated by 120°. While the same is true for the rays of the bright stars at some distance from the center, in the vicinity of the bright center at least one of the double lines is bent by nearly 60°. According to the resulting apparent twist of these stars they are classified (Fig. 2) as c (clockwise) and cc (counterclockwise). The observations so far do not indicate any preference in their appearance or in their distribution across the network. Inspection of Fig. 2 shows finally that the honeycomblike structure is not perfect and in particular that some of the double lines do not meet, but end in a U-turn-like feature (UT). As will be shown below [Fig. 3(c)], the U-turns, like the double lines, are identical with the corresponding features seen on the Au(111) reconstructed surface. Note that the rays ending in a U-turn always originate in a dark star, i.e., the three rays of the bright stars always end in a dark one. All these regularities, as well as the shape of the network itself, originate in the details of the process of the initial formation and further development of the reconstruction network.

The characteristic features of the reconstruction network are shown in more detail in the atomically resolved images in Fig. 3. In the upper left and middle of Fig. 3(a) a dark and a bright star, respectively, are clearly seen. The enlarged image of the bright star in Fig. 3(b) shows that the atomic rows in the central area of the bright star are twisted counterclockwise by about 5°.

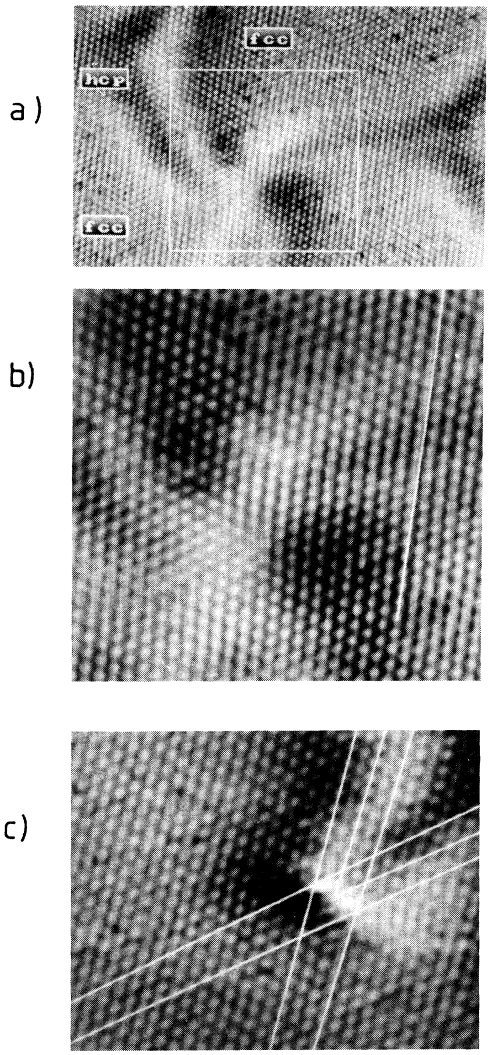

FIG. 3. Atomic resolution STM images after deposition of 0.2 ML at 640 K at a deposition rate of 1×10^{-3} ML/s. (a) Image showing a counterclockwise twisted bright star (middle) and dark stars (upper left and middle right) (scale, 150 Å×110 Å). Areas in which the atoms are located in fcc and hcp positions, respectively, are indicated. (b) Enlarged image of the square marked in (a) (scale 70 Å×70 Å); the straight line evidences the bulging of the Pt atom rows towards the bright star center. (c) Image showing the apex of a U-turn (scale 70 Å×55 Å); the long and short straight lines are intended to help one recognize the disappearance of additional Pt rows at the apex.

This rotation appears to be due to the attempt to relieve the compressive strain which is concentrated in the center of the star. Indeed, as the straight line drawn in Fig. 3(b) emphasizes, the atomic rows within the double lines are bulged towards the bright star center. This being true for each of the double lines which meet in the bright star, the compressive strain is focused into the star. The

compressive strain is apparently so large that the relief by the twisting of the rows is not sufficient so that the topmost atoms in the center of the star are in addition raised by 0.55 Å leading to the brightness of the star.

Finally, Fig. 3(c) demonstrates that the termination of those double lines originating in a dark star which do not end in a bright one has a structure identical to that of the U-turns observed on Au(111) (see, e.g., Fig. 11 in [1]) and modeled in Fig. 10 of Ref. [1]. Indeed, the two pairs of long lines emphasize that two Pt atom rows (marked by the short lines) at an angle of 60° are ending at the apex of the U-turns. This is equivalent to the insertion of one extra atom into each atom row crossing the double lines in the $[1\bar{1}0]$ direction, i.e., to one extra Pt atom along the $[11\bar{2}]$ direction contained in the double line feature. From the estimation of total length of double line per unit area on well developed reconstruction regions, a Pt atom density increase of about 4% in the top layer is obtained. This number has been confirmed in direct experiments by comparing the total amount of Pt atoms contained in Pt islands upon deposition on reconstructed and nonreconstructed areas. The same number has also been found for the high-temperature Pt(111) reconstruction at 1600–1700 K.

From a detailed analysis of atomic resolution images like those in Fig. 3 and in view of the identical structure of the double lines and of the U-turns on Pt and Au we conclude that also on Pt(111) the atoms in the dark regions inside and outside the double lines are located on hcp and fcc sites, respectively [1]. The hcp areas lie about 0.09 ± 0.02 Å higher than the fcc ones, again in fair agreement with the findings on Au(111) [1]. In the bright transition regions and in the center of the bright stars the atoms are located in discommensurate positions, i.e., at a higher level. Further structural details and observations on the kinetics of the reconstruction process will be presented in an extended paper.

In conclusion, we have demonstrated that surface reconstruction can be induced on Pt(111) at temperatures as low as 400 K by increasing the chemical potential of the Pt atom gas phase and that it involves an increased Pt atom density in the top layer in agreement with the theoretical considerations of Needs and co-workers [3,8]. In the absence of the Pt gas phase the lifting of the reconstruction is kinetically hindered up to 700 K.

[1] J. V. Barth, H. Brune, G. Ertl, and R. J. Behm, Phys. Rev. B **42**, 9307 (1990).
[2] A. R. Sandy, S. G. J. Mochrie, D. M. Zehner, G. Grübel, K. G. Huang, and D. Gibbs, Phys. Rev. Lett. **68**, 2192 (1992).
[3] R. J. Needs, M. J. Godfrey, and M. Mansfield, Surf. Sci. **242**, 215 (1991).
[4] K. H. Besocke, Surf. Sci. **181**, 145 (1987).
[5] Th. Michely, Ph.D thesis, Bonn, 1991 (Jül-Bericht No. 2569).
[6] M. Bott, Th. Michely, and G. Comsa, Surf. Sci. **272**, 161 (1992).
[7] H. Niehus and G. Comsa, Surf. Sci. **93**, L147 (1980).
[8] M. Mansfield and R. J. Needs, J. Phys. Condens. Matter **2**, 2361 (1990).

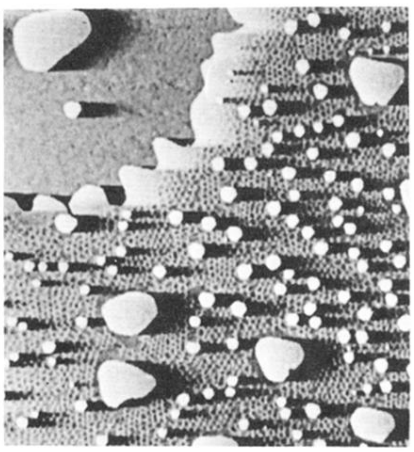

FIG. 1. STM image of 5700 Å×5700 Å taken after deposition of 0.1 ML at 690 K at a deposition rate of 3×10^{-3} ML/s. The image is represented with illumination at near glancing incidence from the left.

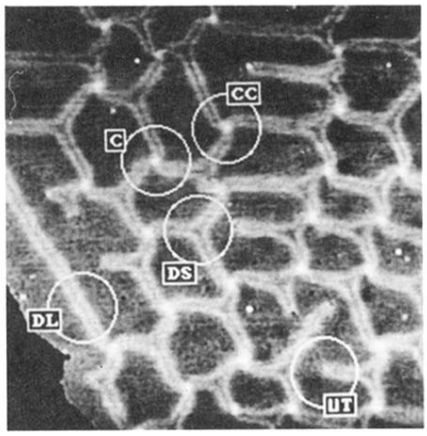

FIG. 2. STM image of 1000 Å × 1000 Å size after deposition of 0.3 ML at 630 K at a deposition rate of 3×10^{-3} ML/s. The higher terrace covering almost the entire image is reconstructed while the lower one (lower left corner) is unreconstructed.

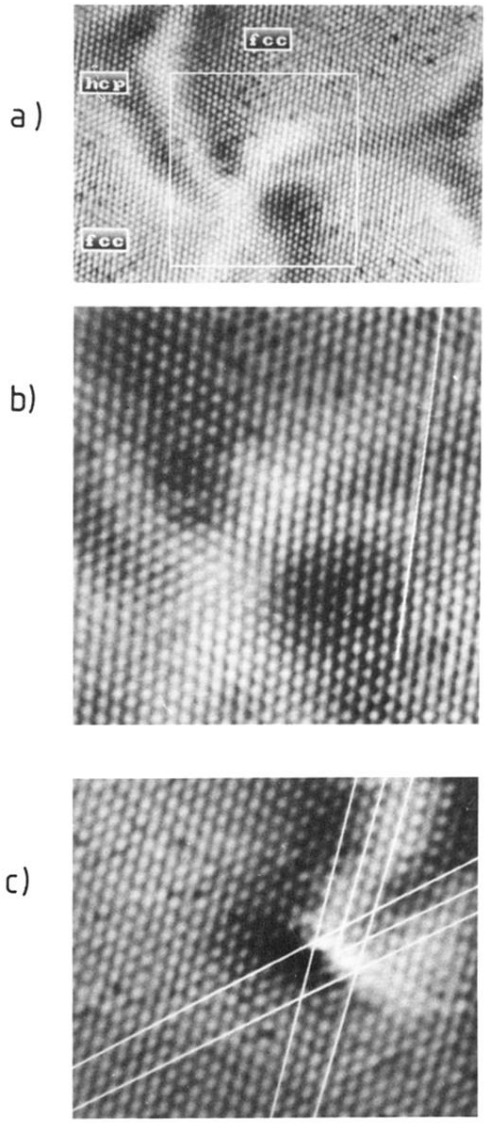

FIG. 3. Atomic resolution STM images after deposition of 0.2 ML at 640 K at a deposition rate of 1×10^{-3} ML/s. (a) Image showing a counterclockwise twisted bright star (middle) and dark stars (upper left and middle right) (scale, 150 Å×110 Å). Areas in which the atoms are located in fcc and hcp positions, respectively, are indicated. (b) Enlarged image of the square marked in (a) (scale 70 Å×70 Å); the straight line evidences the bulging of the Pt atom rows towards the bright star center. (c) Image showing the apex of a U-turn (scale 70 Å×55 Å); the long and short straight lines are intended to help one recognize the disappearance of additional Pt rows at the apex.